ACS SyntheticBiology

pubs.acs.org/synthbio

Research Article

Gold-Specific Biosensor for Monitoring Wastewater Using Genetically Engineered *Cupriavidus metallidurans* CH34

Ssu-Tzu Tsai,[†] Wen-Jui Cheng,[†] Qian-Xian Zhang, and Yi-Chun Yeh*

Cite This: *ACS Synth. Biol.* 2021, 10, 3576−3582

Read Online

ACCESS | Metrics & More | Article Recommendations | Supporting Information

ABSTRACT: Transcription factor-based whole-cell biosensors have recently become promising alternatives to conventional analytical methods due to their advantage of simplicity, cost-effectiveness, and environmental friendliness. In this study, we used genetic engineering to develop a whole-cell biosensor based on the activation of promoters by CupR via interactions with gold ions, leading to the expression of reporter genes that yield output signals. Altering the promoter sequences was shown to significantly improve the performance of the biosensor strain in terms of gold-specificity. The detection sensitivity of our engineered strains was 42-fold higher than that of wild-type strains. The linear range of the purposed sensor was 125−1000 nM with a limit of detection at 46.5 nM. The effectiveness of the sensor strain was verified in wastewater samples.

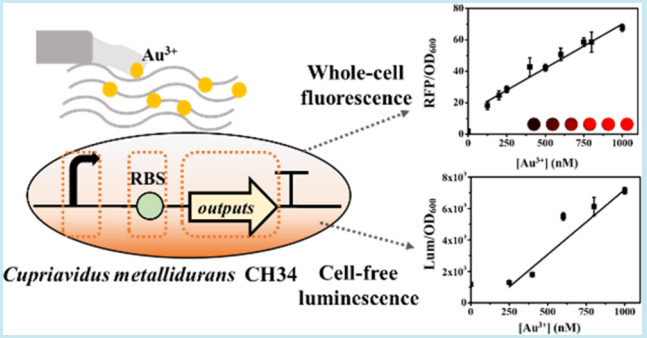

KEYWORDS: *heavy metal, CupR, Cupriavidus metallidurans, gold, whole-cell biosensor*

1. INTRODUCTION

Efficient environmental monitoring requires methods for the rapid and sensitive screening and quantification of environmental pollutants, such as toxic metals. Hazardous heavy metals from contaminated water and soils are potentially toxic. Gold nanoparticles have proven effective as sensing tools or medical diagnostics;[1] however, highly active gold ions (Au(I) and Au(III)) have been shown to damage the human liver, kidney, and nervous system.[2,3] In this current study, we sought to develop a simple and cost-effective approach to monitor gold ions in industrial/electronic wastewater.

Microbial biosensors are a cost-effective alternative approach to monitoring environmental pollutants (e.g., heavy metals, organic pollutants, pathogens, etc.) in minimally equipped settings.[4−10] For example, Styczynski et al. used the pigment expression system to establish a whole-cell biosensor for the visual detection of zinc ions.[11] Microbial biosensors use a natural regulatory circuit within a microorganism to trigger the production of a measurable signal upon sensing the target analyte.[12] A wide range of output signals have been employed in biosensors, including (1) fluorescence proteins, such as red fluorescent protein (mRFP1), green fluorescent protein (GFP), and cyan fluorescent protein (CFP), etc.,[13,14] (2) bioluminescence, such as the luciferase and luciferase subunit (nanoluciferase, Nluc),[14−16] and (3) pigments, such as lycopene,[17] β-carotene,[18] violacein,[19] and betaxanthin.[20] To reduce the cost of purchasing and operating instruments, these output signals are commonly used to achieve reliable reading at a low cost.

The bacteria *Cupriavidus metallidurans* CH34 contains several metal resistance factors, which allow it to survive in areas contaminated by heavy metals.[21] *C. metallidurans* has been shown to perform gold biomineralization via a precipitation process,[22] and MerR family bacterial metal-regulatory protein in *C. metallidurans* (CupR) selectively responds to gold ions.[23,24] Previously, we developed the whole-cell biosensors based on the activation of promoters by CupR via interactions with gold ions, leading to the expression of a reporter gene that yields output signals.[25,26] In this study, we used genetic engineering as a tool to systematically optimize the promoter sequences, ribosome binding sites, and reporting signals to improve the performance of the whole-cell biosensor for the sensitive and selective detection of gold ions in *C. metallidurans*.

2. EXPERIMENTS

2.1. Chemicals. T4 DNA ligase, fast digest enzyme, and phusion DNA polymerase were purchased from Thermo

Received: October 14, 2021
Published: December 3, 2021

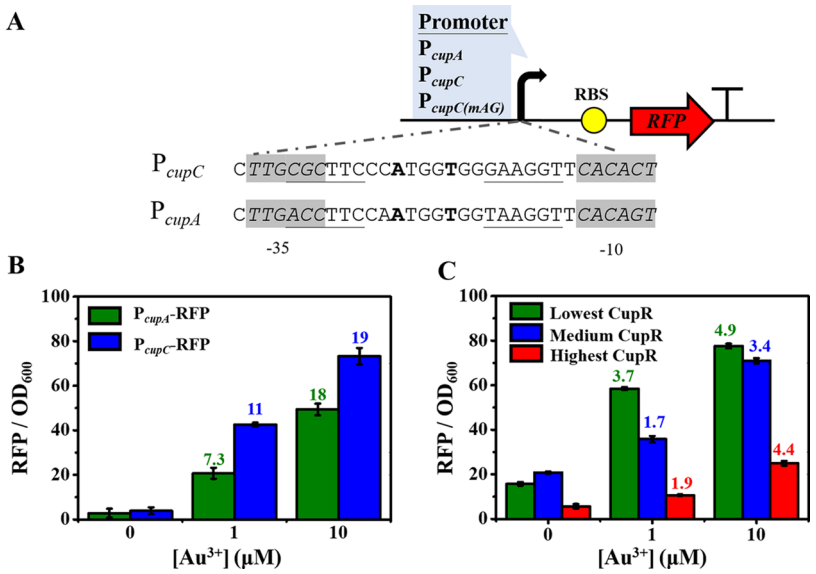

Figure 1. (A) Schematic diagrams of strains used in this study. Arrows indicate the direction of transcription of promoters. RBS indicates ribosomal binding site. Sequences of P_{cupC} and P_{cupA} promoters in *C. metallidurans* CH34. The predicted −10 and −35 elements are highlighted in gray. The symmetric dyad sequences are underlined. The bold fonts represent the 3′ and 3 sites. (B) RFP intensity/OD_{600} ratios of two CupR-regulated promoters (P_{cupA} and P_{cupC}) in the presence (1 and 10 μM) and absence of gold ions 24 h post induction. (C) Comparison of RFP intensity/OD_{600} ratios between three biosensors expressing various amounts of CupR proteins in the presence (1 and 10 μM) and absence of gold ions 24 h post induction. P_{BAD}-cupR strain was induced with 0.4% arabinose. Values were the induction folds relative to the uninduced controls. Error bars represent the SD (standard deviation) of three independent experiments (n = 3).

Scientific (Waltham, MA). The Presto Mini Plasmid Kit and Gel/PCR DNA Fragments Kit were purchased from Geneaid Biotech Ltd. (New Taipei city, Taiwan). BugBuster protein extraction reagent and furimazine were purchased from Merck (Darmstadt, Germany) and AOBIOUS INC. (Gloucester, MA), respectively.

2.2. Cloning and Construct Assembly. *E. coli* DH5α is the host strain used to construct various strains with standard procedures. It was inoculated in LB broth at 37 °C overnight in a shaker (250 rpm). *C. metallidurans* cells were used as the host for whole-cell biosensor and incubated at 28 °C in NaCl-free LB (SLB) with shaking at 200 rpm. Standard protocols for conjugation with *E. coli* strain S17 were used to generate *C. metallidurans* CH34 strains.[27] The primers, plasmids, strains, and construct details are provided in Tables S1, S2, and S3.

2.3. Metal Ion Inductions. A single colony was initially cultured in LB broth and grown overnight at 28 °C on a rotatory shaker at 200 rpm. The cells were then diluted (4%) in an SLB medium. The SLB medium contains 10 g/L tryptone (VWR life science) and 5 g/L yeast extract (VWR life science). The SLB medium was supplemented with kanamycin at 200 μg/mL (AMRESCO) and gentamicin at 15 μg/mL (AMRESCO). The cells were diluted in the SLB medium and incubated at 28 °C on a rotatory shaker at 200 rpm (OD_{600} = 0.4). Then, we added metal ions to induce the expression of the output signals.

2.4. Measurement of Optical Density and Fluorescence. At the end of the reaction, 300 μL of the sample was used to determine fluorescence. The cells were centrifuged at 14 000*g* for 1 min and washed with 300 μL of phosphate-buffered saline (PBS). Next, red fluorescence intensity (ex: 530 nm, em: 590 nm) and OD were recorded with a BioTek Synergy HT instrument in a 96-well plate.

For luminescence measurements, the cells were centrifuged at 14 000*g* for 1 min, and the supernatant was discarded. Fifty microliters of BugBuster protein extraction reagent was added to the pellet to redissolve it and then quickly mixed with 50 μL of BugBuster containing 100 μM substrate. The bioluminescence was recorded using a BioTek Synergy HT instrument (em: 485 nm, the integration time is 0.5 ms, and the gain value at 135).

2.5. Preparation of Wastewater Samples. Municipal wastewater was collected from local sewage treatment factories from a local wastewater treatment plant. Municipal wastewater was centrifuged and filtered before ICP-MS analysis. All measurements were accomplished using an iCAP TQ (Thermo Scientific). Then, wastewater was mixed with 2XSLB at a ratio of 1:1 as our culture medium using whole-cell and cell-free methods. $HAuCl_4$ was spiked in the medium with standard addition methods.

3. RESULTS AND DISCUSSION

3.1. Construction of a Gold-Responsive Whole-Cell Biosensor in *C. metallidurans*. We first compared the activity of two CupR-responsive promoters (P_{cupC} and P_{cupA}) in terms of fluorescence intensity (RFP/OD_{600}) at 24 h post induction with gold ions (0, 1, and 10 μM). The promoter sequence alignment of P_{cupC} and P_{cupA} are presented in Figure 1A. Two sensor strains containing identical plasmids were employed for the specific detection of gold ions using the red fluorescent protein (RFP) gene as a reporter driven by P_{cupC} or P_{cupA}. Relative to green and cyan fluorescent proteins, RFPs are beneficial for imaging under autofluorescence conditions. The cells carrying P_{cupC} presented higher induction upon incubation with gold ions (Figure 1B). We constructed a strain with a native (P_{cupR}) or inducible promoter (P_{BAD}) to drive the expression of CupR to indirectly estimate CupR protein levels using RFP fluorescence as the reporter. We first examined the promoter strength by constructing P_{cupR}-RFP and P_{BAD}-RFP. The two promoters were activated using gold

https://doi.org/10.1021/acssynbio.1c00520
ACS Synth. Biol. 2021, 10, 3576−3582

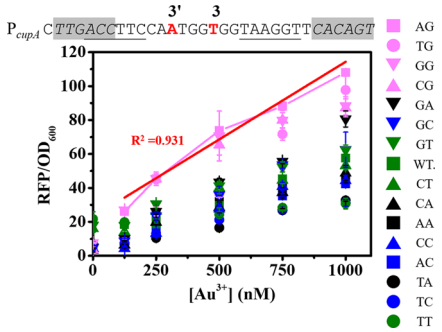

Figure 2. RFP intensity/OD_{600} ratios of 16 mutants that were created using altered nucleotide compositions at the 3′ and 3 operator positions of P_{cupA} AN, TN, CN, and GN (N: A, T, C, G) in the presence of gold ions (0, 125, 250, 500, 750, 1000 nM) in the SLB medium 24 h post induction. Error bars represent the SD (standard deviation) of three independent experiments (n = 3). RFP intensity intensity/OD_{600} exhibited an excellent linear correlation with the gold ion concentration for $P_{cupA(mAG)}$ strain in the range of 100−1000 nM (R^2 = 0.931).

ions or arabinose at various concentrations, respectively (Figure S1). Activation of the P_{BAD} promoter was 37-fold stronger than that of the native P_{cupR} promoter based on the RFP intensities. We then compared the activation of P_{cupC} at three CupR concentration levels (lowest to highest: CupR expressed by the endogenous chromosomal locus, exogenous expression by the P_{cupR}-cupR, exogenous expression by the P_{BAD}-cupR) in the presence of 1 or 10 μM gold ions and 0.4% arabinose. We observed no significant difference in cell density (OD_{600}) due to the toxicity of the gold ions at those concentrations. Note that the expression of RFP was significantly higher when the expression of CupR was lower (Figure 1C). Thus, we adopted the strain with lower CupR expression for subsequent experiments based on high-signal intensities.

3.2. Optimizing the Nucleotide Composition at the 3′ and 3 Operator Positions of P_{cupA}. Audero et al. reported that CupR homologues (CueR and GolS) are able to selectively distinguish target binding sites by recognizing bases at positions 3′ and 3 of their cognate operators.[28−30] They also reported C/A conserved at the 3′ position and G/T at the 3 position (relative to the center of the operator) in *E. coli*/*Salmonella*. Thus, we performed saturation mutagenesis to create all possible 16 mutants at the 3′ and 3 operator positions (Figure S2A) and recorded the fluorescence intensity/OD_{600} in the presence of gold ions (0, 125, 250, 500, 750, 1000 nM). We first examined the effect at the 3 position by comparing four groups carrying mAN, mTN, mCN, and mGN (m: mutation sites; N: any nucleotide) using mAG as a reference (Figure S2B−E). The mAG mutant presented the strongest reactivity to gold ions. We found that the increase in fluorescence intensity in the presence of gold ions was most pronounced when the 3 position was G (Figure S2B−E). The dose−response curves between the fluorescence intensity/OD_{600} of 16 strains and gold concentrations are plotted in Figure 2.

It has previously been demonstrated that sequences at the 3′ and 3 operator positions can amend specificity toward regulators.[28−30] Thus, we tested strains carrying mAN and mNG in the presence of an interfering substance (e.g., Ag and Cu) using a wild-type sequence (AT)-based biosensor as a control. In Figures 3 and S3, the fluorescence intensity/OD_{600} values were then respectively examined in the presence of three metal ions (Au, Ag, and Cu). None of the biosensors responded to Ag at tested concentrations. The strain carrying mGG presented the strongest induction in the presence of Cu ions. We then calculated an Au/Cu discrimination index based

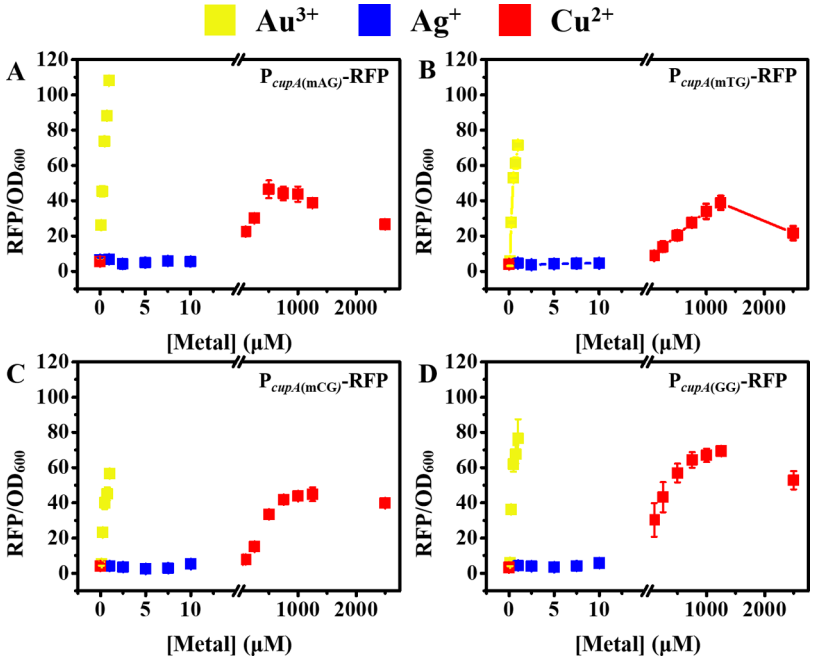

Figure 3. Red fluorescence profiles of whole-cell biosensor strains carrying mutated nucleotide composition (mAG, mTG, mCG, and mGG) at the 3′ and 3 operator positions of P_{cupA} in the presence of gold, silver, and copper ions at various concentrations in the SLB medium (gold: 0, 125, 250, 500, 750, 1000 nM, silver: 0, 1, 2.5, 5, 7.5, 10 μM, and copper: 0, 100, 250, 500, 750, 1000, 1250, 2500 μM). Error bars represent the SD (standard deviation) of three independent experiments (n = 3).

https://doi.org/10.1021/acssynbio.1c00520
ACS Synth. Biol. 2021, 10, 3576−3582

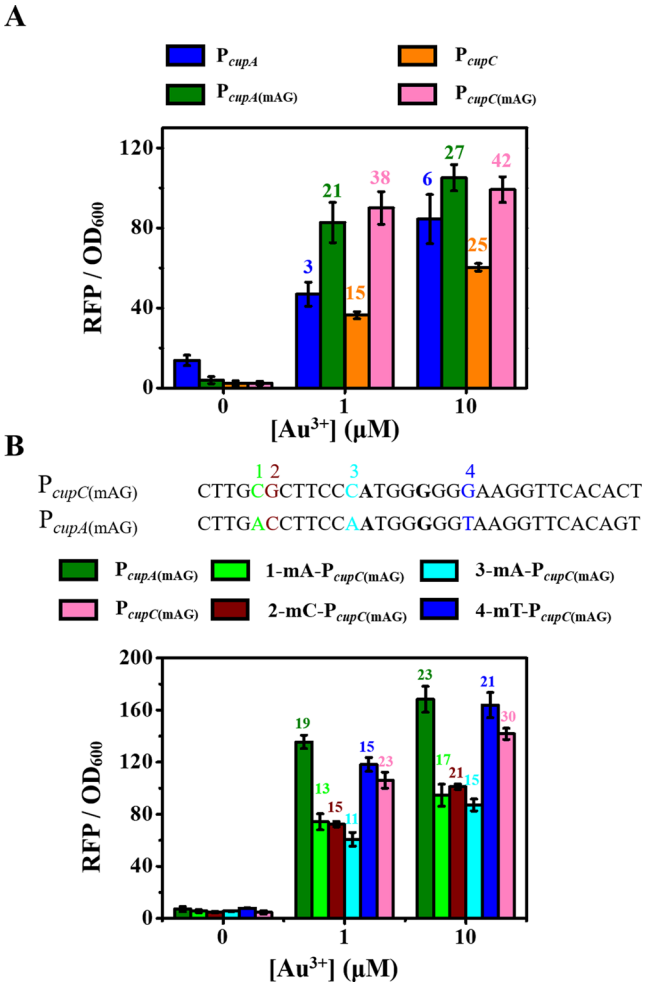

Figure 4. (A) RFP intensity/OD_{600} ratios of strains carrying P_{cupA} or P_{cupC} with or without mutations (mAG) at the 3′ and 3 operator positions in the presence (1 and 10 μM) and absence of gold ions 24 h post induction. (B) Sequence comparison between P_{cupC} and P_{cupA}. The RFP intensity/OD_{600} ratios of six strains in the presence (1 and 10 μM) and absence of gold ions 24 h post induction. The values above the bars indicate the fold induction compared to control. Error bars represent the SD (standard deviation) of three independent experiments (n = 3).

on the ratio of the maximum induction attained with Au and Cu ions (Table S4). The strain carrying mAG presented in the highest specificity to gold ions (stronger induction with gold ion than copper ions). The mAG mutant exhibited 2.33 times

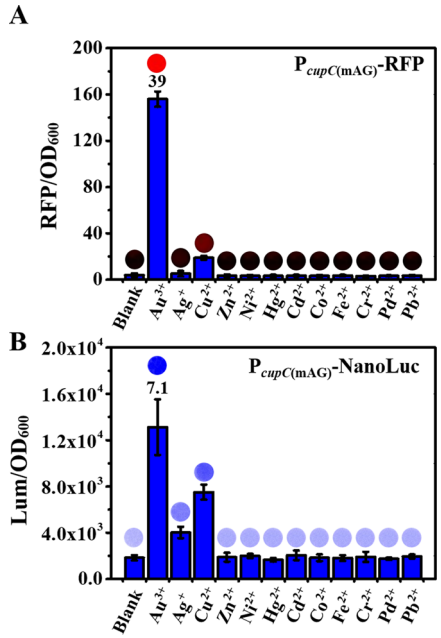

Figure 6. (A) Red fluorescent intensity and images of the purposed whole-cell and (B) luminescence intensity and images of the cell-free biosensors in the presence of various heavy metals at the concentration of 10 μM, except for Cu^{2+} and Zn^{2+}, which were added at a concentration of 100 μM due to their relative abundance in environmental samples at 24 and 6 h post induction. Error bars represent the standard deviation from triplicate measurements. The values above the bars indicate the fold induction compared to control.

better discrimination between Cu and Au than wild-type, which can be attributed to the interaction strength between DNA and CupR. We, therefore, selected A at the 3′ position and G at the 3 position for subsequent development.

3.3. Promoter, Growth Phase, and RBS Effects on Biosensor Performance. We used two promoter sequences with or without mutations at the 3′ and 3 positions (P_{cupA}, P_{cupA}(mAG), P_{cupC}, P_{cupC}(mAG)) to verify the enhancements of mAG and again observed increases in fluorescence intensity resulting from the mutations at 3′ and 3 positions (Figure 4A). In fact, two of the promoter sequences led to 2−7-fold increases in fluorescence intensity with mAG mutations. The P_{cupC} also presented higher inductions than those of P_{cupA} due to very low basal reporter gene expression, which was consistent with our comparison of P_{cupC} and P_{cupA}.

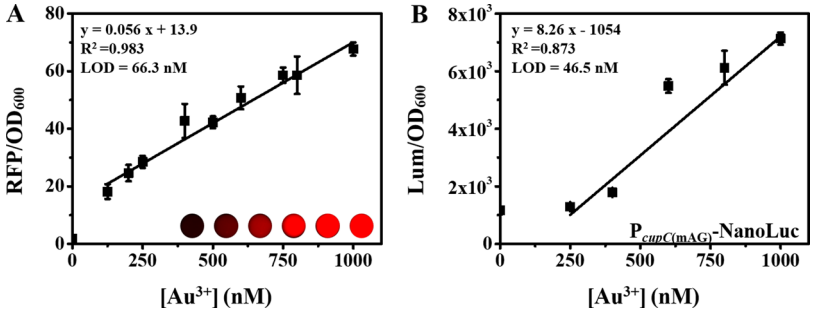

Figure 5. Linear relationships between the concentration of gold ions (0, 250, 400, 600, 800, 1000 nM) and the intensity of (A) red fluorescence and (B) luminescence were plotted. LODs were 66.3 and 46.5 nM, respectively. Error bars represent the SD (standard deviation) of three independent experiments (n = 3).

https://doi.org/10.1021/acssynbio.1c00520
ACS Synth. Biol. 2021, 10, 3576−3582

We then investigated how promoter sequences affected the expression of the basal reporter gene. Pairwise alignment of P_{cupC} and P_{cupA} promoter revealed highly similar sequences except for four nucleotides. We performed single nucleotide substitutions, which involved exchanging the nucleotide of promoter P_{cupC} with P_{cupA}. Four strains were constructed by substituting C, G, C, and G to A, C, A, and T at positions 1, 2, 3, and 4 of P_{cupC}, respectively, named 1-mA, 2-mC, 3-mA, and 4-mT (Figure 4B). A subsequent comparison of four strains with native promoters (P_{cupA} and P_{cupC}) revealed that switching these positions did not have a significant effect on the responses to gold ions in terms of induction folds and intensities (Figure 4B).

Considering that fluorescence intensity was enhanced in the presence of gold ions, we sought to determine whether the gold-induced response was affected by the growth phase. This was achieved by following the reaction time-course of cells during exponential and stationary growth phases (Figure S4A). We observed a linear relationship between fluorescence intensity/OD_{600} and gold ion concentration in the range of 125−1000 nM during the exponential growth phase (at 12 h post induction). The cells induced during the stationary phase (at 9 h post induction) also presented a significant increase in fluorescence. The increase in fluorescence did not vary significantly between growth phases. This means that sensitivity could be increased simply by extending gold ions' exposure time, and exposure time could be shortened when monitoring samples with a high gold ion concentration.

We then evaluated a set of RBS sequences for controlling RFP in terms of translation initiation efficiency in *C. metallidurans*. These included four previously reported RBS sequences known to have high translation initiation efficiency (RBS_{30}, RBS_{34}, RBS_{nrdD}, and RBS_{cal}),[31,32] and one was calculated using the software published by Salis et al.[33] ($RBS_{mRFP1.cal}$). The detailed sequences of RBSs are listed in Table S5. Again, we observed a strong correlation between fluorescence intensity and gold ion concentrations in all strains. RBS_{nrdD} and RBS_{cal} presented the lowest signal intensity and induction folds. $RBS_{mRFP1.cal}$ presented the strongest intensity; however, the induction fold was less pronounced than that of RBS_{30} (Figure S5). Thus, we adopted the RBS_{30} sequence as our optimal gold-responsive platform due to its high efficiency and low leaky expression of the reporter.

3.4. Employing Nanoluciferase as the Signal Reporter. Bioluminescent cell-free biosensors have been applied for environmental testing or on-site analysis with portable devices.[34−36] We thus sought to reduce the reaction time by replacing RFP with a bioluminescent enzyme (Nluc). Bioluminescence was recorded under lysing conditions using furimazine substrates (50 μM) at 6 h post induction with gold ions. As shown in Figure 5B, luminescence intensity/OD_{600} exhibited an excellent linear correlation with the gold ion concentration in the range of 250−1000 nM (R^2 = 0.983). These results indicate that comparable detection sensitivity could be achieved with shorter reaction times using a cell-free system (Figure 5A).

3.5. Selectivity of Purposed Sensor Strain toward Heavy Metals. We also investigated potential sources of interference by measuring selectivity for common heavy metals in whole-cell and cell-free systems. This involved incubating sensor cells in the exponential phase with various metal ions at the concentration of 10 μM, except for Cu^{2+} and Zn^{2+}, which were added at a concentration of 100 μM due to their relative abundance in environmental samples. We observed a significant increase in red fluorescence intensity in the presence of gold ions. The other metals (including Ag, Zn, Ni, Hg, Cd, Co, Fe, Cr, Pd, and Pb) did not induce significant changes in red fluorescence (Figure 6A). In the presence of 100 μM copper, the luminescence increased slightly, while the other metal ions only resulted in minor changes in luminescence, thereby demonstrating the high specificity of the proposed biosensors (Figure 6B).

3.6. Performance of the Proposed Sensor Strain in Wastewater. Finally, we evaluated the purposed biosensors in municipal wastewater collected from a local wastewater treatment plant. Note that all samples were confirmed to be free of gold based on ICP-MS measurements (shown in Table S6). Table S6 lists the quantitative results for the detection of two-spiked samples in a 50% wastewater matrix using whole-cell and cell-free methods. As shown in Table S7, the average recovery rates and RSD range from 82 to 118% and from 1 to 11%, respectively. Our results indicate that the purposed whole-cell and cell-free biosensors could potentially be used to assess the toxicity of gold-polluted wastewater samples.

4. CONCLUSIONS

In this study, we systematically investigated promoters, ribosome binding sites, and reporter signals with the aim of enhancing the sensitivity and selectivity of whole-cell gold biosensors capable of high-throughput environment monitoring. Specifically, we successfully enhanced the performance of the whole-cell biosensor by the fine-tuning affinity of the transcription factor module via alterations of the sequence of operators. We genetically engineered the nonmodel organism *C. metallidurans* for growth in extreme environments to expand the scope and applicability of the biosensors. To overcome a longer doubling time (e.g., slower growth), this cell-free platform could be developed in parallel to reduce the time required for detection.

■ ASSOCIATED CONTENT

Supporting Information

The Supporting Information is available free of charge at https://pubs.acs.org/doi/10.1021/acssynbio.1c00520.

Experimental details Table S1−5, metal contents of wastewater determined by ICP-MS and cell-based method (Table S6 and S7), mutant characterizations (Figures S1−3), the time-trace fluorescence intensity (Figure S4), and RBS characterizations (Figure S6) (PDF)

■ AUTHOR INFORMATION

Corresponding Author

Yi-Chun Yeh − *Department of Chemistry, National Taiwan Normal University, Taipei 116, Taiwan;* orcid.org/0000-0002-8267-0360; Phone: +886277496117; Email: yichuny@ntnu.edu.tw; Fax: +886229324249

Authors

Ssu-Tzu Tsai − *Department of Chemistry, National Taiwan Normal University, Taipei 116, Taiwan*

Wen-Jui Cheng − *Department of Chemistry, National Taiwan Normal University, Taipei 116, Taiwan*

Qian-Xian Zhang − *Department of Chemistry, National Taiwan Normal University, Taipei 116, Taiwan*

https://doi.org/10.1021/acssynbio.1c00520
ACS Synth. Biol. 2021, 10, 3576−3582

Complete contact information is available at:
https://pubs.acs.org/10.1021/acssynbio.1c00520

Author Contributions

†S-T.T. and W.-J.C. contributed equally to this work. Y.C.Y. designed the research; S.T.T., W.J.C., and Q.X.Z. performed the experiments; all authors participated in analyzing the data and writing the paper.

Notes

The authors declare no competing financial interest.

■ ACKNOWLEDGMENTS

This work was funded by the Ministry of Science and Technology of Taiwan under the project number 107-2113-M-003−013-MY3 and 110-2113-M-003-009-. This work was also financially supported by the National Taiwan Normal University (NTNU) within the framework of the Higher Education Sprout Project by the Ministry of Education (MOE) in Taiwan. The authors thank Wen-Feng Chang at Instrumentation Center of National Tsing Hua University for the ICP-MS analysis.

■ REFERENCES

(1) Daniel, M.-C.; Astruc, D. Gold Nanoparticles: Assembly, Supramolecular Chemistry, Quantum-Size-Related Properties, and Applications toward Biology, Catalysis, and Nanotechnology. *Chem. Rev.* **2004**, *104*, 293−346.

(2) Block, W. D.; Knapp, E. L. Metabolism, Toxicity, and manner of action of gold compounds in the treatment of arthritis, VII. The effect if carious gold compoimds on the oxygen consumption of rat tissues. *J. Pharmacol. Exp. Ther.* **1945**, *83*, 275−278.

(3) Habib, A.; Tabata, M. Oxidative DNA damage induced by HEPES (2-[4-(2-hydroxyethyl)-1-piperazinyl] ethanesulfonic acid) buffer in the presence of Au (III). *J. Inorg. Biochem.* **2004**, *98*, 1696−1702.

(4) Saeidi, N.; Wong, C. K.; Lo, T. M.; Nguyen, H. X.; Ling, H.; Leong, S. S.; Poh, C. L.; Chang, M. W. Engineering microbes to sense and eradicate *Pseudomonas aeruginosa*, a human pathogen. *Mol. Syst. Biol.* **2011**, *7*, 521.

(5) Guo, M.; Wang, J.; Du, R.; Liu, Y.; Chi, J.; He, X.; Huang, K.; Luo, Y.; Xu, W. A test strip platform based on a whole-cell microbial biosensor for simultaneous on-site detection of total inorganic mercury pollutants in cosmetics without the need for predigestion. *Biosens. Bioelectron.* **2020**, *150*, No. 111899.

(6) King, J. M.; Digrazia, P. M.; Applegate, B.; Burlage, R.; Sanseverino, J.; Dunbar, P.; Larimer, F.; Sayler, G. S. Rapid, sensitive bioluminescent reporter technology for naphthalene exposure and biodegradation. *Science* **1990**, *249*, 778−781.

(7) Whangsuk, W.; Thiengmag, S.; Dubbs, J.; Mongkolsuk, S.; Loprasert, S. Specific detection of the pesticide chlorpyrifos by a sensitive genetic-based whole cell biosensor. *Anal. Biochem.* **2016**, *493*, 11−13.

(8) Belkin, S.; Yagur-Kroll, S.; Kabessa, Y.; Korouma, V.; Septon, T.; Anati, Y.; Zohar-Perez, C.; Rabinovitz, Z.; Nussinovitch, A.; Agranat, A. J. Remote detection of buried landmines using a bacterial sensor. *Nat. Biotechnol.* **2017**, *35*, 308−310.

(9) Wei, W.; Zhu, T.; Wang, Y.; Yang, H.; Hao, Z.; Chen, P. R.; Zhao, J. Engineering a gold-specific regulon for cell-based visual detection and recovery of gold. *Chem. Sci.* **2012**, *3*, 1780−1784.

(10) He, M.-Y.; Lin, Y.-J.; Kao, Y.-L.; Kuo, P.; Grauffel, C.; Lim, C.; Cheng, Y.-S.; Chou, H.-H. D. Sensitive and specific cadmium biosensor developed by reconfiguring metal transport and leveraging natural gene repositories. *ACS Sens.* **2021**, *6*, 995−1002.

(11) McNerney, M. P.; Michel, C. L.; Kishore, K.; Standeven, J.; Styczynski, M. P. Dynamic and tunable metabolite control for robust minimal-equipment assessment of serum zinc. *Nat. Commun.* **2019**, *10*, No. 5514.

(12) Park, D. M.; Taffet, M. J. Combinatorial Sensor Design in *Caulobacter crescentus* for Selective Environmental Uranium Detection. *ACS Synth. Biol.* **2019**, *8*, 807−817.

(13) Hsu, L.-W.; Lin, Y.-H.; Guo, J.-Y.; Chen, C.-F.; Chou, Y.-J.; Yeh, Y.-C. Simultaneous Determination of l-Phenylalanine, Phenylethylamine, and Phenylacetic Acid Using Three-Color Whole-Cell Biosensors within a Microchannel Device. *ACS Appl. Bio Mater.* **2020**, *3*, 5120−5125.

(14) Lopreside, A.; Wan, X.; Michelini, E.; Roda, A.; Wang, B. Comprehensive Profiling of Diverse Genetic Reporters with Application to Whole-Cell and Cell-Free Biosensors. *Anal. Chem.* **2019**, *91*, 15284−15292.

(15) Hall, M. P.; Unch, J.; Binkowski, B. F.; Valley, M. P.; Butler, B. L.; Wood, M. G.; Otto, P.; Zimmerman, K.; Vidugiris, G.; Machleidt, T.; Robers, M. B.; Benink, H. A.; Eggers, C. T.; Slater, M. R.; Meisenheimer, P. L.; Klaubert, D. H.; Fan, F.; Encell, L. P.; Wood, K. V. Engineered luciferase reporter from a deep sea shrimp utilizing a novel imidazopyrazinone substrate. *ACS Chem. Biol.* **2012**, *7*, 1848−1857.

(16) Dixon, A. S.; Schwinn, M. K.; Hall, M. P.; Zimmerman, K.; Otto, P.; Lubben, T. H.; Butler, B. L.; Binkowski, B. F.; Machleidt, T.; Kirkland, T. A.; Wood, M. G.; Eggers, C. T.; Encell, L. P.; Wood, K. V. NanoLuc Complementation Reporter Optimized for Accurate Measurement of Protein Interactions in Cells. *ACS Chem. Biol.* **2016**, *11*, 400−408.

(17) McNerney, M. P.; Styczynski, M. P. Precise control of lycopene production to enable a fast-responding, minimal-equipment biosensor. *Metab. Eng.* **2017**, *43*, 46−53.

(18) Watstein, D. M.; McNerney, M. P.; Styczynski, M. P. Precise metabolic engineering of carotenoid biosynthesis in *Escherichia coli* towards a low-cost biosensor. *Metab. Eng.* **2015**, *31*, 171−180.

(19) Guo, Y.; Hui, C.-y.; Liu, L.; Chen, M.-p.; Huang, H.-y. Development of a bioavailable Hg(II) sensing system based on MerR-regulated visual pigment biosynthesis. *Sci. Rep.* **2021**, *11*, No. 13516.

(20) Chou, Y.-C.; Shih, C.-I.; Chiang, C.-C.; Hsu, C.-H.; Yeh, Y.-C. Reagent-free DOPA-dioxygenase colorimetric biosensor for selective detection of L-DOPA. *Sens. Actuators, B* **2019**, *297*, No. 126717.

(21) Monchy, S.; Benotmane, M. A.; Wattiez, R.; Van Aelst, S.; Auquier, V.; Borremans, B.; Mergeay, M.; Taghavi, S.; Van der Lelie, D.; Vallaeys, T. Transcriptomic and proteomic analyses of the pMOL30-encoded copper resistance in *Cupriavidus metallidurans* strain CH34. *Microbiology* **2006**, *152*, 1765−1776.

(22) Funari, R.; Ripa, R.; Söderström, B.; Skoglund, U.; Shen, A. Q. Detecting Gold Biomineralization by Delftia acidovorans Biofilms on a Quartz Crystal Microbalance. *ACS Sens.* **2019**, *4*, 3023−3033.

(23) Fang, C.; Philips, S. J.; Wu, X.; Chen, K.; Shi, J.; Shen, L.; Xu, J.; Feng, Y.; O'Halloran, T. V.; Zhang, Y. CueR activates transcription through a DNA distortion mechanism. *Nat. Chem. Biol.* **2021**, *17*, 57−64.

(24) Jian, X.; Wasinger, E. C.; Lockard, J. V.; Chen, L. X.; He, C. Highly Sensitive and Selective Gold(I) Recognition by a Metalloregulator in *Ralstonia metallidurans*. *J. Am. Chem. Soc.* **2009**, *131*, 10869−10871.

(25) Guo, K.-H.; Chen, P.-H.; Lin, C.; Chen, C.-F.; Lee, I.-R.; Yeh, Y.-C. Determination of gold ions in human urine using genetically engineered microorganisms on a paper device. *ACS Sens.* **2018**, *3*, 744−748.

(26) Tseng, H.-W.; Tsai, Y.-J.; Yen, J.-H.; Chen, P.-H.; Yeh, Y.-C. A fluorescence-based microbial sensor for the selective detection of gold. *Chem. Commun.* **2014**, *50*, 1735−1737.

(27) Deng, Y.; Zhang, X.; Zhang, X. Recent advances in genetic modification systems for Actinobacteria. *Appl. Microbiol. Biotechnol.* **2017**, *101*, 2217−2226.

(28) Pérez Audero, M. E.; Podoroska, B. M.; Ibáñez, M. M.; Cauerhff, A.; Checa, S. K.; Soncini, F. C. Target transcription binding sites differentiate two groups of MerR-monovalent metal ion sensors. *Mol. Microb.* **2010**, *78*, 853−865.

(29) Humbert, M. V.; Rasia, R. M.; Checa, S. K.; Soncini, F. C. Protein signatures that promote operator selectivity among paralog MerR monovalent metal ion regulators. *J. Biol. Chem.* **2013**, *288*, 20510−20519.
(30) Pontel, L. B.; Audero, M. E. P.; Espariz, M.; Checa, S. K.; Soncini, F. C. GolS controls the response to gold by the hierarchical induction of *Salmonella*-specific genes that include a CBA efflux-coding operon. *Mol. Microbiol.* **2007**, *66*, 814−825.
(31) Wang, B.; Kitney, R. I.; Joly, N.; Buck, M. Engineering modular and orthogonal genetic logic gates for robust digital-like synthetic biology. *Nat. Commun.* **2011**, *2*, No. 508.
(32) Bi, C.; Su, P.; Müller, J.; Yeh, Y.-C.; Chhabra, S. R.; Beller, H. R.; Singer, S. W.; Hillson, N. J. Development of a broad-host synthetic biology toolbox for *Ralstonia eutropha* and its application to engineering hydrocarbon biofuel production. *Microb. Cell Fact.* **2013**, *12*, No. 107.
(33) Espah Borujeni, A.; Channarasappa, A. S.; Salis, H. M. Translation rate is controlled by coupled trade-offs between site accessibility, selective RNA unfolding and sliding at upstream standby sites. *Nucleic Acids Res.* **2014**, *42*, 2646−2659.
(34) Roda, A.; Cevenini, L.; Michelini, E.; Branchini, B. R. A portable bioluminescence engineered cell-based biosensor for on-site applications. *Biosens. Bioelectron.* **2011**, *26*, 3647−3653.
(35) Cevenini, L.; Calabretta, M. M.; Lopreside, A.; Tarantino, G.; Tassoni, A.; Ferri, M.; Roda, A.; Michelini, E. Exploiting NanoLuc luciferase for smartphone-based bioluminescence cell biosensor for (anti)-inflammatory activity and toxicity. *Anal. Bioanal. Chem.* **2016**, *408*, 8859−8868.
(36) Esimbekova, E. N.; Kalyabina, V. P.; Kopylova, K. V.; Torgashina, I. G.; Kratasyuk, V. A. Design of bioluminescent biosensors for assessing contamination of complex matrices. *Talanta* **2021**, *233*, No. 122509.

https://doi.org/10.1021/acssynbio.1c00520
ACS Synth. Biol. 2021, 10, 3576−3582